APPENDIX B

Publication P9

Repo A.-K., Rasilo P., Niemenmaa A., Arkkio A. Identification of electromagnetic torque model for induction machines with numerical magnetic field solution", *IEEE Transactions on Magnetics*, in press.

Identification of Electromagnetic Torque Model for Induction Machines with Numerical Magnetic Field Solution

Anna-Kaisa Repo, Paavo Rasilo, Asko Niemenmaa, and Antero Arkkio

Abstract— **The identification of a parametric electromagnetic torque model for induction machines is studied. The data for the identification procedure is provided by the numerical impulse response test performed within a two-dimensional time-stepping finite element analysis (FEA). The parametric models are obtained from the theory of electric machines. The parameters are estimated using the data obtained from the numerical field solution. Within the impulse test, an assumption of linear behaviour in the neighbourhood of an operation point is made. As the real electric machine is a nonlinear, time-variant system, the applicability of the impulse test is studied by several means.**

Index Terms—**Finite element methods, Frequency response, Induction machines, Parameter estimation.**

I. Introduction

An electric machine converts mechanical energy to the electric one, or vice versa. The machine is always a part of a power transmission. Mechanical and electrical properties of the connection depend on the type of the machine, but forced and free torsional oscillations exist inherently. For example, in power production such oscillations may occur as an energy-flow fluctuation in a wind farm [1] and mechanical vibration in diesel generating units [2]. Traditionally, torsional oscillations have been analyzed with low-order analytical models [3], and recently with high-order finite element models [4]. A moderate compromise between time-consuming, high-order models and simple low-order models can be achieved by proper parameter estimation.

The aim of this paper is to present a simple parametric model for the dynamic electromagnetic torque of induction machines. The model depicts the response of the electromagnetic torque to the torsional perturbations in the rotor angle. This model can be combined with a mechanical torsion model to build an electromechanical system model.

Manuscript received June 24, 2007. This work was supported by the Graduate School of Electrical Engineering GSEE, Finnish Funding Agency for Technology and Innovation TEKES, ABB Oy, Kone Oyj, and High Speed Tech Ltd.

A.-K. Repo is with Helsinki University of Technology, P.O. Box 3000 (phone: +358-09-4512381; fax: +358-09-4512991; e-mail: anna-kaisa.repo@tkk.fi).

P. Rasilo is with Helsinki University of Technology (e-mail: paavo.rasilo@tkk.fi).

A. Niemenmaa is with Helsinki University of Technology (e-mail: asko.niemenmaa@tkk.fi).

A. Arkkio is with Helsinki University of Technology (e-mail: antero.arkkio@tkk.fi).

II. Methods

A. Numerical impulse response test

In mechanics, impulse response tests are used to identify vibration characteristics of structures. The structure is excited by an impulse and the response of the system is measured. Both the excitation and response signals are converted to the frequency domain and from their ratio the frequency response function (FRF) is computed. A numerical method very similar to the mechanical impulse test has been successfully applied to identify electromagnetic force models [5].

This study is focused on modeling torsional oscillations. Hence, the impulse excitation is applied to the rotor position angle. The impulse test is performed within a 2D time-stepping finite-element analysis which includes the magnetic saturation, skin effect in the rotor bars and rotation of the slotted rotor. The time-step of the FE analysis is 50 μs. The impulse is presented in Fig. 1. The amplitude is exaggerated for illustration purposes.

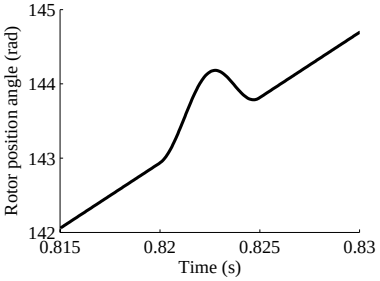

Fig. 1. Impulse excitation applied to the rotor angle.

At the beginning of the impulse test, the machine is operating at the steady state. The impulse is applied to the rotor angle and the machine is simulated until the response of the torque has completely decayed. Typically, 20 000 time-steps are sufficient. The impulse to the angle and the response of the electromagnetic torque are converted to the frequency domain using Discrete Fourier Transform (DFT). From their ratio, the FRF of the electromagnetic torque is obtained.

The impulse should excite all the frequencies in the

frequency range studied. The length of the impulse defines the frequency contents obtained. For example, an impulse of length 5.0 ms has a nonzero frequency contents up to 400 Hz [6]. By shortening the length of the impulse, a wider frequency range can be studied. However, in the case of the speed oscillations, the frequency range of 0…100 Hz is usually adequate. The electric machine produces certain frequencies within its normal operation. In order to distinguish the impulse response, the steady state has to be cancelled. This can be performed by computing the same operation point without any impulse excitation and subtracting the results from the perturbed case.

The FRF can be obtained also by exciting every frequency under interest separately and computing the corresponding response. The method is referred as harmonic excitation. The procedure is otherwise similar to the impulse test but every point in the FRF requires a separate computation. Since the electromagnetic torque is assumed to be a linear function of the rotor angle, the FRFs obtained by the harmonic excitation and the impulse test should coincide. Another method to evaluate the applicability of the impulse test is to study the effect of the amplitude of the impulse. In the case of a linear time-invariant system, the amplitude does not influence the shape of the FRF. When a nonlinear system is linearized around an operation point, the magnitudes of excitation signal for which the assumption of linearity holds have to be defined. Empirically, this can be done by performing several impulse tests and increasing the amplitude of impulse gradually. When the shape of the resulting FRF begins to deteriorate, the assumption of linearity is not valid anymore.

B. Small-signal models

The slip-ring machines and cage-induction machines differ from the rotor. The slip-ring machine is magnetized also from the rotor side and the rotor is constructed from filamentary conductors. The rotor of the cage-induction machine has deep rotor bars which are short-circuited. Thus, two different circuit models are needed: T-equivalent circuit model for slip-ring machines and a double-cage model for cage-induction machines.

The models are presented in Fig. 2. The parameters of the T-equivalent circuit are: stator and rotor resistances R_s and R_{r1}, magnetizing inductance L_m, and stator and rotor leakage inductances $L_{\sigma s}$ and $L_{\sigma r1}$. To obtain the double-cage model, the resistance of another parallel rotor branch R_{r2} and the common leakage inductance L_c between the stator and rotor are included. In this case, $\underline{u}_r$ is zero. In Fig. 2, the parameters related to the double-cage model are circumscribed. In the T-equivalent circuit, $L_c = 0$ and $R_{r2} = \infty$.

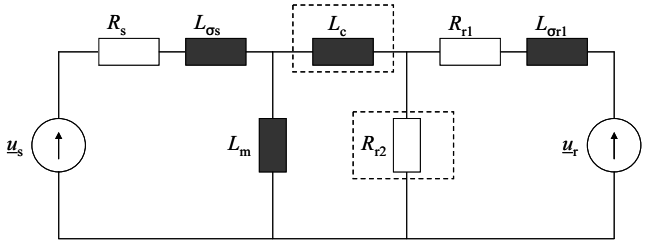

Fig. 2. The circuit models used in parameter estimation. T-equivalent circuit is used for slip-ring machines and modified double-cage model for cage-induction machines (extra parameters circumscribed).

The small-signal models are derived from the space-vector theory. The currents are chosen as free variables and the flux linkage equations are substituted in voltage equations. In order to use real-valued variables, the equations are separated into real and imaginary parts. Thus, a corresponding analytical small-signal model is derived by assuming small perturbations around the steady-state rotor position angle, electromagnetic torque and currents. The steady-state quantities are subtracted and the products of perturbations are neglected. The small-signal equations for the T-equivalent circuit in the synchronous frame of reference rotating at speed ω_k (superscript *k* refers to the reference frame) are

$$\Delta\underline{u}_s^k = R_s\Delta\underline{i}_s^k + \frac{\mathrm{d}\Delta\underline{\psi}_s^k}{\mathrm{dt}} + \mathrm{j}\omega_k\Delta\underline{\psi}_s^k \tag{1}$$

$$\Delta\underline{u}_r^k = R_r\Delta\underline{i}_r^k + \frac{\mathrm{d}\Delta\underline{\psi}_r^k}{\mathrm{dt}} + \mathrm{j}\left(\omega_k - \omega_r - \frac{\mathrm{d}\Delta\theta_r}{\mathrm{dt}}\right)\Delta\underline{\psi}_r^k \tag{2}$$

$$\Delta\underline{\psi}_s^k = \left(L_m + L_{\sigma s}\right)\Delta\underline{i}_s^k + L_m\Delta\underline{i}_r^k \tag{3}$$

$$\Delta\underline{\psi}_r^k = L_m\Delta\underline{i}_s^k + \left(L_m + L_{\sigma r}\right)\Delta\underline{i}_r^k \tag{4}$$

$$\Delta T_e = \frac{3}{2}pl_m\left[\mathrm{conj}\left(\underline{i}_{r0}^k\right)\Delta\underline{i}_s^k + \underline{i}_{s0}^k\mathrm{conj}\left(\Delta\underline{i}_r^k\right)\right]. \tag{5}$$

$\underline{i}_{s0}{}^k = i_{sx0}{}^k + \mathrm{j}i_{sy0}{}^k$ and $\underline{i}_{r0}{}^k = i_{rx0}{}^k + \mathrm{j}i_{ry0}{}^k$ are the steady-state currents. In order to use real-valued quantities, (1)–(5) are separated into real and imaginary parts. The small-signal model for a double-cage circuit is derived similarly [8].

During the impulse test, the stator and rotor voltage supplies are kept constant. For cage-induction machine $\Delta\underline{u}_r = 0$, but in the case of a slip-ring machine the rotor voltage is perturbed along with the rotor position angle. Here, the dependence between the rotor voltage and angle is assumed linear so that $\Delta\underline{u}_r{}^k = \underline{k}\Delta\theta_r$, where $\underline{k}$ is a complex-valued coefficient. Eqs. (3) and (4) are substituted in (1) and (2) and the time-derivatives are replaced by Laplace-variable *s*. From those, the current components as a function of rotor angle can be solved. When these are substituted in (5), the electromagnetic torque as a function of rotor position angle in frequency domain is obtained. In the rest of the paper, the superscript *k* is left away for simplicity.

C. Parameter estimation

The numerical data is fitted to small-signal model using Differential Evolution [10]. In addition to the circuit parameters, the small-signal models contain steady-state current components i_{sx0}, i_{sy0}, i_{rx0}, and i_{ry0}. Moreover, in the case of the double-cage model the total rotor current consists of two sub-currents $i_{rx0} = i_{r1x0} + i_{r2x0}$ and $i_{ry0} = i_{r1y0} + i_{r2y0}$. Some of the parameters may depend on each other and cannot all be estimated. On the other hand, a good fit is obtained when as many parameters as possible are allowed to vary. The presented procedure is adopted by trying different alternatives and selecting the one that gives the best results.

The stator current can be obtained from the steady-state time-stepping analysis. Reasonable steady-state estimates for $L_{\sigma s}$ and L_m (R_s is known) can be obtained from time-harmonic FEA [11]. From these parameters and the stator voltage and current, the total rotor current can be solved. In the case of the slip-ring machine, the amplitude of rotor current is fixed to this value. i_{rx0} is estimated and i_{ry0} is calculated from that and the fixed amplitude. In addition, the components of $\underline{k}$ are also estimated. The ratio of $L_{\sigma r1}$ and $L_{\sigma s}$ is fixed to the value given by the time-harmonic analysis. For the cage-induction machine, the total rotor current is calculated similarly and both the components are fixed. The current components i_{r1x0} and i_{r1y0} are estimated and i_{r2x0} and i_{r2y0} are calculated from the estimates and the total rotor current. $L_{\sigma r1}$ is calculated from the estimate of $L_{\sigma s}$ and the fixed ratio of the stator and total rotor leakage inductance [8].

III. Results

A. Applicability of the impulse test

1.7-MW slip-ring and cage-induction machines are studied. The type of the slip-ring machine is common in wind-power applications. The stator windings of the machines are similar. The supply voltage is 690 V delta-connected and the supply frequency is 50 Hz. The stator and rotor temperatures are 100 °C. The cage-induction machine is operating in motor regime at slip 1.2 %. The slip-ring machine is used as a generator at slip –12 %. Next, the results obtained for the slip-ring machine are presented.

The amplitude of the impulse is varied between 1…80 % of the pole pitch. Fig. 3 presents the FRFs obtained with relative amplitudes of 5, 20 and 50 %. The harmonic excitation with the relative amplitude of 5 % is performed at some frequencies. Fig. 4 presents the comparison between the FRFs obtained by the impulse test and the harmonic excitation.

Since both the rotor position angle and electromagnetic torque are real-valued signals, the negative side of the FRF is a complex conjugate of the positive side. The poles are at 50 Hz and at the slip frequency, 6 Hz. Since the FRF is defined from the rotor angle, the imaginary part represents the electromagnetic damping and the real part the spring constant [3]. It should be noted that within the ranges of 0…6 Hz and 37…50 Hz the imaginary part is positive indicating negative electromagnetic damping. This means that when the machine is connected to a mechanical system, instabilities or torsional oscillations may occur. The effects of negative damping for induction machines have been studied in [9].

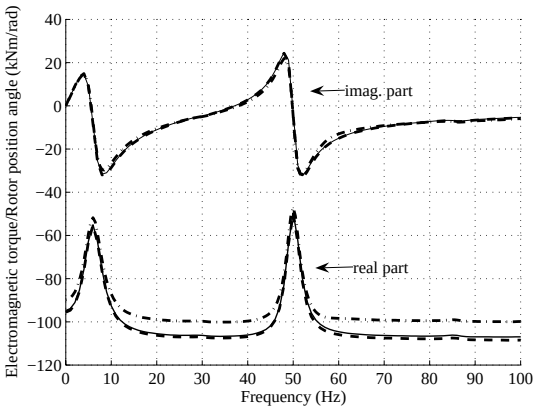

Fig. 3. FRFs for the slip-ring machine obtained using the relative impulse amplitude of 5 % (solid line), 20 % (dashed), and 50 % (dashed-dotted).

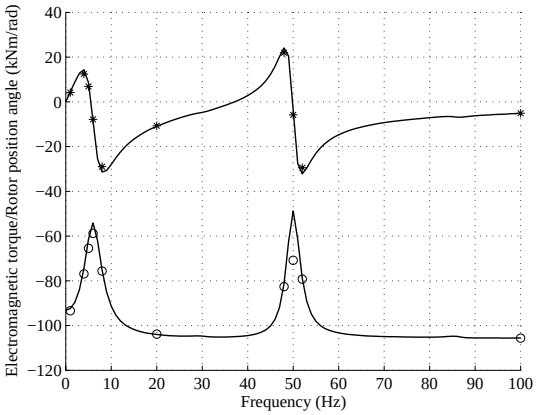

Fig. 4. FRFs for the slip-ring machine obtained using the impulse test and the harmonic excitation (real part o, imag. part *).

B. Parameter estimates

Fig. 5 shows the fit for the induction machine. The fit obtained for the slip-ring machine is equally good. Table 1 shows the estimated parameters for both the machines. The components of the currents and coefficient $\underline{k}$ are aligned with respect to the real-valued stator voltage. The fixed parameters are denoted by asterisk and the parameters calculated from the fixed and the estimated parameters during the estimation are denoted by two asterisks.

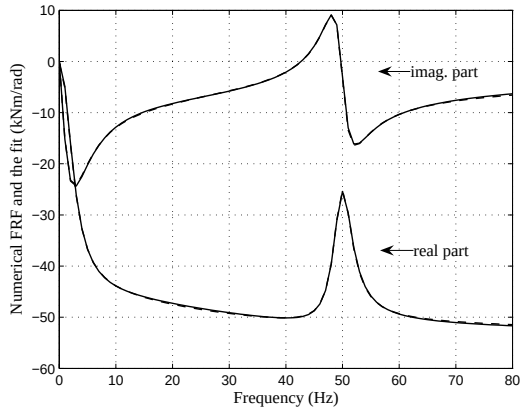

Fig. 5. Numerical FRF (solid) and the fitted FRF (dashed) for the cage-induction machine.

TABLE I
PARAMETER ESTIMATES

parameter	unit	slip-ring	cage-ind.
r_s	[mΩ]	2.12*	2.12*
$l_{\sigma s}$	[mH]	0.124	0.0949
l_m	[mH]	2.85	2.60
$l_{\sigma r1}$	[mH]	0.0648**	2.65**
r_{r1}	[mΩ]	2.80	4.68
l_c	[mH]	/	0.0674
r_{r2}	[mΩ]	/	5.62
Re($\underline{k}$)	[V/rad]	21.5	/
Im($\underline{k}$)	[V/rad]	75.5	/
i_{sx0}	[A]	–1660*	2200*
i_{sy0}	[A]	–280*	–1270*
i_{rx0}	[A]	1830	–2310*
i_{ry0}	[A]	918**	630*
i_{r1x0}	[A]	/	5450
i_{r1y0}	[A]	/	–2190
i_{r2x0}	[A]	/	–7760**
i_{r2y0}	[A]	/	2810**

* Fixed to a constant value
** Calculated during the estimation from the fixed parameters and estimates

By substituting the parameter estimates in the analytical small-signal models the transfer functions can be obtained. The transfer function for the slip-ring machine is

$$\frac{\Delta T_e(s)}{\Delta\theta_r(s)} = \frac{\left[s-(-5.18+\mathrm{j}313.8)\right]\left[s-(-5.18-\mathrm{j}313.8)\right]}{\left[s-(-8.02+\mathrm{j}37.00)\right]\left[s-(-8.02-\mathrm{j}37.00)\right]} \cdot \frac{\left[s-(-11.29+\mathrm{j}313.7)\right]\left[s-(-11.29-\mathrm{j}313.7)\right]}{\left[s-(-15.23+\mathrm{j}37.24)\right]\left[s-(-15.23+\mathrm{j}37.24)\right]} \quad (6)$$

and for the cage-induction machine

$$\frac{\Delta T_e(s)}{\Delta\theta_r(s)} = \frac{\left[s-(-6.39+\mathrm{j}313.7)\right]\left[s-(-6.39-\mathrm{j}313.7)\right]}{\left[s-(-12.79+\mathrm{j}313.0)\right]\left[s-(-12.79-\mathrm{j}313.0)\right]} \cdot \frac{\left[s-(-12.98)\right]\left[s-(-184.0)\right]\left[s-(-217.6)\right]s}{\left[s-(-14.50+\mathrm{j}4.29)\right]\left[s-(-14.50+\mathrm{j}4.29)\right]} \cdot \frac{1}{\left[s-(-214.8+\mathrm{j}4.40)\right]\left[s-(-214.8+\mathrm{j}4.40)\right]} \quad (7)$$

IV. DISCUSSION

Based on the computations, it can be concluded that the response of the electromagnetic torque is a linear function of the relative rotor position angle within the range 1…20 %. The comparison between the FRFs obtained from the impulse test and the harmonic excitation show a good agreement. For both of the machine types, the fits are very good and the circuit-parameter estimates are physically reasonable.

Transfer functions (6) and (7) differ by the order and structure. For the cage-induction machine, a higher-order model is needed. An impulse excitation to the rotor angle induces current harmonics to the rotor bars in a wide frequency range. Thus, the influence of skin effect becomes more significant than at steady-state operation associated with low rotor frequencies.

The slip-ring machine the rotor of which is supplied from a voltage source effectively works as a synchronous machine. The torque response at DC is high. This property is included in the analytical model (1)–(5) by the rotor-voltage perturbation linearly proportional (by coefficient $\underline{k}$) to the rotor-angle perturbation. From (7) and Fig. 5 it can be seen that for the cage-induction machine the torque response is zero at $s = 0$. This is reasonable since the torque of cage-induction machines is not affected by the position of the steady-state rotor angle.

In reality, the dynamic behavior of rotating machines is time-variant. Thus, the numerical FRF and parameter estimates of the time-invariant analytical model may depend on the time instant when the impulse test is performed. The effects of time-dependency will be the subject of future study.

REFERENCES

[1] Tabesh, A., Iravani, R.: "Small-signal dynamic model and analysis of a fixed-speed wind farm – a frequency response approach", IEEE Trans. On Power Delivery, 21(2): 778–787, 2006.
[2] Craighead, I.A., Gray, T.G.F.: "Investigation of diesel generator shaft and bearing failures", Proc. Instn. Mesh. Engrs., Part K: J. Multi-body Dynamics, 218:153–158, 2004.
[3] Kovacs, P.K.: "Transient Phenomena in Electrical Machines", Elsevier, 1984.
[4] Arkkio, A., Westerlund, J.: "An electromechanical model for analysing transients in diesel-driven synchronous generators", Proc. Int. Conf. on Electrical Machines, 2:878–882, 2000.
[5] Holopainen, T.P.: "Electromechanical interaction in rotor dynamics of cage induction motors", Doctoral Thesis, Helsinki University of Technology, 2004.
[6] Ewins, D.J.:"Modal testing: theory, practice and application", 2nd edition, Research studies press Ltd. England, 2000.
[7] Melkebeek, J.A.A., Novotny, D.W.: "The Influence of Saturation on Induction Machine Drive Dynamics", IEEE Trans. Ind. Appl., Vol. IA-19, No. 5, September/October 1983, pp. 671–681.
[8] Repo, A.-K., Arkkio, A.: " Numerical impulse response test to identify parametric models for closed-slot deep-bar induction motors", IET Proc – Electric Power Applications, Vol. 1, No. 3, May 2007, pp. 307–315.
[9] Concordia, C.: "Induction motor damping and synchronizing torques", AIEE Transactions Power Apparatus and Systems, Vol. 71, January 1952, pp. 364–366.
[10] Price, K.V., Storn, R.M., Lampinen, J.A.: "Differential evolution: a practical approach to global optimization", Springer Berlin, 2005.
[11] Arkkio, A.: "Analysis of induction motors based on the numerical solution of the magnetic field and circuit equations", Doctoral Thesis, Helsinki University of Technology, 1987.